Available online at www.sciencedirect.com

ScienceDirect

Mendeleev Commun., 2020, **30**, 654–656

Mendeleev Communications

Direct UVC photodegradation of imipramine in aqueous solutions: a mechanistic study

Ekaterina D. Mordvinova,[a,b] Olga A. Snytnikova,[a,c] Victoria A. Salomatova,[a,b] Vadim V. Yanshole,[a,c] Vyacheslav P. Grivin[a,b] and Ivan P. Pozdnyakov*[a,b]

[a] *Novosibirsk State University, 630090 Novosibirsk, Russian Federation. E-mail: ipozdnyak@kinetics.nsc.ru*
[b] *V. V. Voevodsky Institute of Chemical Kinetics and Combustion, Siberian Branch of the Russian Academy of Sciences, 630090 Novosibirsk, Russian Federation*
[c] *International Tomography Center, Siberian Branch of the Russian Academy of Sciences, 630090 Novosibirsk, Russian Federation*

DOI: 10.1016/j.mencom.2020.09.034

Mechanism of direct UVC photolysis of dibenzazepine-type drug imipramine (IMI) was revealed by the combination of laser flash photolysis for the detection of short lived intermediates and steady-state photolysis coupled with LC-MS for identification of final products. Both quantum yield of IMI photoionization and molar absorption coefficient of IMI radical cation were determined for the first time.

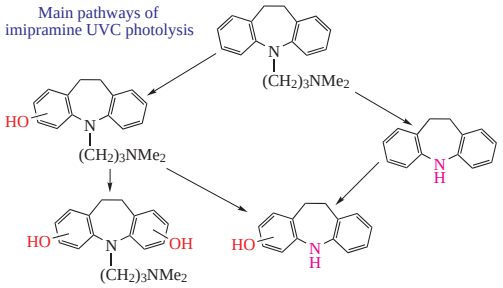

Keywords: pharmaceuticals, dibenzazepines, antidepressants, UVC photolysis, laser flash photolysis, photodegradation, radicals, photoionization, water treatment.

Pharmaceuticals and personal care products (PPCPs) are among most of widespread persistent contaminants in environment[1] and great attention is paid now to development of different techniques for their decomposition including photochemical ones.[2] Tricyclic antidepressants (TAs) belong to PPCPs and are widely used for treatment of different diseases, including depression, anxiety and a variety of chronic pain syndromes. These compounds are quite resistant to common wastewater treatment procedures, so they have been extensively detected in surface waters and soils.[3–5] One of the urgent questions is a fate of TAs under influence of solar light (λ > 290 nm) in natural waters or during UVC treatment (λ < 290 nm) of TA containing wastewaters.

Published data on TA photodegradation in water is scarce. Generally, direct UVC (254 nm) photolysis of these compounds[6–9] or combination of UV irradiation with addition of hydrogen peroxide,[6–9] potassium persulfate,[8,10] chlorine,[8] Fe^{II}/Fe^{III} ions[6] or titanium dioxide TiO_2[11] were applied. Direct photolysis of TAs in water exhibits low quantum yields (1.4% for nortriptyline and 0.76% for amitriptyline) and leads to the products of hydroxylation, deamination and side chain elimination.[6,9] The presence of chemical additives and photocatalysts enhances the degradation of TAs due to generation of reactive radicals ($Cl^{\bullet-}$, $SO_4^{\bullet-}$ and $^{\bullet}OH$). Under optimal conditions, complete mineralization of TAs and organic photoproducts can be achieved.[11] However, detailed mechanisms of photoreactions and identification of short lived intermediates are absent in aforesaid works. There is only one work[12] in which mechanism of photolysis of a set of imipramine (IMI) derivatives was studied in different solvents by laser flash photolysis (LFP, λ_{ex} = 266 nm) and fluorescence techniques. It was assumed that initial photoprocess in water was the photoionization with the formation of radical cation and hydrated electron.

Finally, it was shown that TAs amitriptyline and nortriptyline underwent indirect photodegradation in the presence of the fulvic acid.[13] The mechanism of photodegradation was proposed including electron transfer between the triplet state of the fulvic acid and TAs, similar for other amine drugs.[14,15] The electron transfer could take place in a complex between fulvic acids and TAs as it was demonstrated recently by fluorescence spectroscopy.[16]

The goal of the current work was to reveal the mechanism of direct UVC photolysis of dibenzazepine-type TA, namely imipramine (IMI), 5-(3-dimethylaminopropyl)-10,11-dihydro-5*H*-dibenzo[*b*,*f*]azepine, by LFP, steady-state photolysis and LC-MS technique (for experimental details, see Online Supplementary Materials and refs. 17,18). The main attention was paid to the identification of short-lived intermediates and final photoproducts and to the determination of quantum yields of both primary species and IMI photolysis. This data could be important for further understanding of TAs photodegradation in processes of UVC disinfection.

Flash (266 nm) excitation of IMI aqueous air-equilibrated solutions leads to formation of transient absorption (Figure 1) belonging to two intermediates in accordance with the reported data.[12] First short-lived intermediate exhibits maximum absorbance at 720 nm and its lifetime increases from 0.17 to 2.5 μs after removal of dissolved oxygen, being characteristic of hydrated electron.[19] The second one is not sensitive to the presence of dissolved oxygen (lifetime is about 100 μs) and demonstrates absorption maximum at 680 nm[12] (see Figure 1, spectrum at delay of 8.5 μs).

Therefore, excitation of IMI leads to its photoionization with the formation of a hydrated electron (e_{aq}^-)–radical cation ($IMI^{+\bullet}$) pair.[12] Yields of both species from excitation energy could be

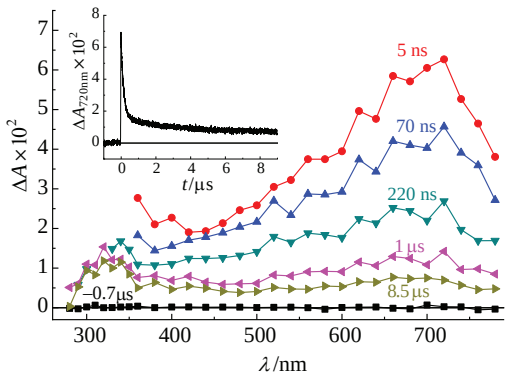

Figure 1 Laser flash (266 nm, 1.7 mJ per pulse) photolysis of air-equilibrated IMI (5×10^{-4} mol dm^{-3}) solutions. Transient absorption spectra at different time delays between excitation and probing pulses are shown. Note that some points at short delays (5–220 ns) are omitted due to an artefact created by scattered excitation pulse. Inset shows a kinetic curve at 720 nm.

calculated using two-exponential fits at 680 and 720 nm, respectively [Figure 2(*a*)], according to the following equation:

$$\Delta A = A(\lambda, e_{aq}^-) \exp(-t/\tau_1) + A(\lambda, IMI^{+\bullet}) \exp(-t/\tau_2), \quad (1)$$

where λ is a registration wavelength (680 or 720 nm); $A(\lambda, e_{aq}^-)$ and $A(\lambda, IMI^{+\bullet})$ are absorption amplitudes at $t = 0$ for e_{aq}^- and $IMI^{+\bullet}$, respectively; τ_1 and τ_2 are observed lifetimes of e_{aq}^- and $IMI^{+\bullet}$, respectively.

The quantum yield of the hydrated electron is not sensitive to both initial IMI (10^{-5}–10^{-4} mol dm^{-3}) or dissolved oxygen concentration and it is equal to (8 ± 0.8)%. Linear dependence of $A(680, IMI^{+\bullet})$ on $A(720, e_{aq}^-)$ allows one to determine molar absorption coefficient of $IMI^{+\bullet}$, $\varepsilon(680, IMI^{+\bullet}) = (5.3 \pm 1.0) \times 10^4$ dm^2 mol^{-1} [Figure 2(*b*)] using published value of $\varepsilon(720, e_{aq}^-) = 2.27 \times 10^5$ dm^2 mol^{-1}.[20] Both photoionization quantum yield and absorption coefficient of the radical cation were determined for the first time. So, in primary stage of IMI photolysis in air-saturated solution the formation of two main intermediates, $IMI^{+\bullet}$ and superoxide radical anion are expected:

$$IMI \xrightarrow{h\nu} IMI^{+\bullet} + e_{aq}^- \quad (2)$$

$$e_{aq}^- + O_2 \xrightarrow{h\nu} O_2^{-\bullet} \qquad k = 2 \times 10^{10} \text{ dm}^3 \text{ mol}^{-1} \text{ s}^{-1} \text{ (ref. 19)} \quad (3)$$

Products and efficiency of IMI photodegradation were determined by steady-state photolysis (254 nm) with HPLC separation and UV detection [Figure 3(*a*)]. Quantum yield of

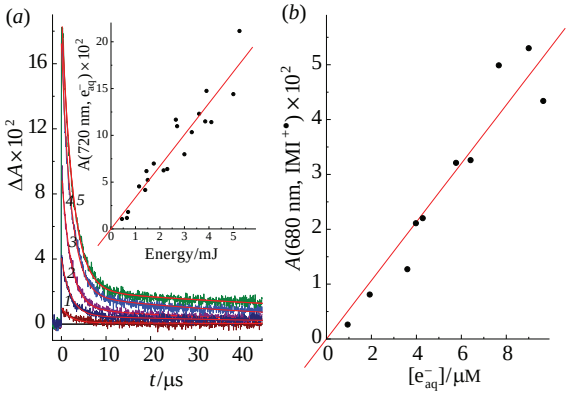

Figure 2 Laser flash (266 nm) photolysis of argon-saturated IMI (5.3×10^{-4} mol dm^{-3}) solutions. (*a*) Kinetic curves at 720 nm, excitation energy (*1*) 0.3, (*2*) 1.4, (*3*) 2.3, (*4*) 4.2 and (*5*) 5.2 mJ per pulse. Solid curves are the best fits using equation (1). Inset is the dependence of A(720 nm, e_{aq}^-) upon excitation energy. (*b*) The dependence of A(680 nm, $IMI^{+\bullet}$) on concentration of hydrated electron.

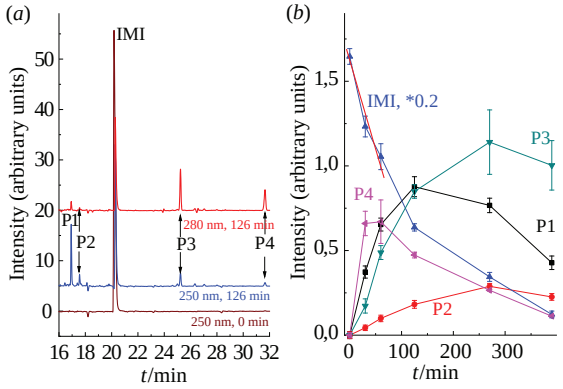

Figure 3 Steady state (254 nm, 0.15 J min^{-1}) photolysis of air-equilibrated IMI (8×10^{-6} mol dm^{-3}) solutions. (*a*) UV chromatograms at 250 and 280 nm for non-irradiated sample and sample after 126 min of UVC irradiation. (*b*) Change of integral peak intensity of IMI and main photoproducts during photolysis. Straight line is the best linear fit used for calculation of IMI photodegradation quantum yield. Note that intensity for IMI was multiplied by factor 0.2 for better visualization.

IMI UVC photolysis is rather low, $\phi^{254} = (3.3 \pm 0.5) \times 10^{-3}$ in agreement with reported findings[6,9] and 90% removal of the drug takes more than 350 min of UVC irradiation. Degradation of IMI leads to four main photoproducts (Scheme 1, Table 1), which exhibits red-shifted absorption up to 500 nm (see Online Supplementary Materials, Figure S1). Among them P4 is the primary photoproduct which is very sensitive to photolysis and P1–P3 demonstrate more resistance to the direct photodegradation than IMI as could be seen from HPLC data [Figure 3(*b*)]. Based on chemical formulae of photoproducts determined by the high-resolution LC-MS technique (see Table 1) and their kinetic behavior the following mechanism of IMI photolysis was proposed (see Scheme 1).

The radical cation of IMI undergoes either side chain elimination leading to P4 or oxidative hydroxylation [by dissolved oxygen or by $O_2^{-\bullet}$ formed in reaction (3)] with formation of P2 (hydroxylated IMI). Both P2 and P4 are sensitive to secondary photolysis and give products P3 (hydroxylated IMI without side chain) and P1 (doubly hydroxylated IMI) in the same main photoprocesses (see Scheme 1). These products are

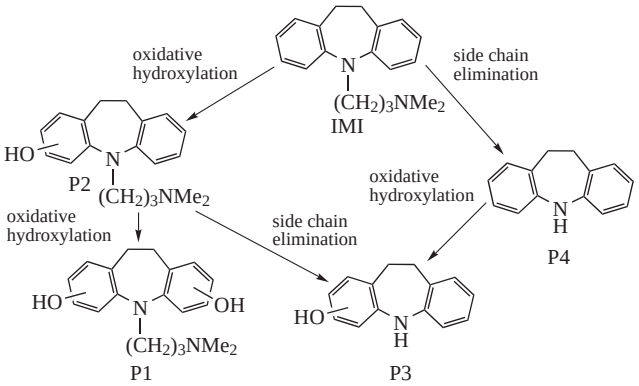

Scheme 1

Table 1 Main products of IMI photolysis in air-equilibrated aqueous solution.

Retention time/min	Measured ion mass $[M + H]^+(m/z)$	Theoretical ion mass $[M + H]^+(m/z)$	Acronym and theoretical molecular formula
16.9	313.1913	313.1911	P1, $C_{19}H_{24}N_2O_2$
17.6	297.1961	297.1961	P2, $C_{19}H_{24}N_2O$,
20.2	281.2013	281.2012	IMI, $C_{19}H_{24}N_2$
25.2	212.1066 210.0911 ($-H_2$)	212.1070 210.0913 ($-H_2$)	P3, $C_{14}H_{13}NO$
31.6	196.1123	196.1121	P4, $C_{14}H_{13}N$

also not photostable [see Figure 3(*b*)], however their photooxidation proceeds very slowly and this was not investigated in the work.

In conclusion, the combination of laser flash photolysis and high-resolution LC-MS techniques allowed us to establish the mechanism of direct UVC photolysis of IMI in aqueous solution. Primary stage is the photoionization with the formation of radical cation–hydrated electron pair. The latter species is rapidly converted to the superoxide radical anion in presence of dissolved oxygen. The radical cation would undergo oxidative hydroxylation and side chain elimination leading to four main photoproducts. This data could be important for understanding the fate of IMI and similar TAs in the processes of UVC disinfection.

The work was supported by the Russian Foundation for Basic Research (grant no. 18-53-00002_BEL) and the Belarusian Republican Foundation for Fundamental Research (grant no. F18R-140). Authors also thank Ministry of Science and Higher Education of the RF for funding the access to MS equipment.

Online Supplementary Materials

Supplementary data associated with this article can be found in the online version at doi: 10.1016/j.mencom.2020.09.034.

References

1 V. Calisto and V. I. Esteves, *Chemosphere*, 2009, **77**, 1257.
2 Y. Yang, Y. S. Ok, K.-H. Kim, E. E. Kwon and Y. F. Tsang, *Sci. Total Environ.*, 2017, **596**–**597**, 303.
3 D. R. Baker, V. Očenášková, M. Kvicalova and B. Kasprzyk-Hordern, *Environ. Int.*, 2012, **48**, 28.
4 H. Li, M. W. Sumarah and E. Topp, *Environ. Toxicol. Chem.*, 2013, **32**, 509.
5 A. Lajeunesse, S. A. Smyth, K. Barclay, S. Sauve and C. Gagnon, *Water Res.*, 2012, **46**, 5600.
6 F. J. Real, F. J. Benitez, J. L. Acero, G. Roldan and F. Casas, *Ind. Eng. Chem. Res.*, 2012, **51**, 16209.
7 F. J. Benitez, J. L. Acero, F. J. Real, G. Roldan and E. Rodriguez, *Water Res.*, 2013, **47**, 870.
8 F. J. Benitez, F. J. Real, J. L. Acero and F. Casas, *Int. J. Chem. Mol. Nucl. Mat. Met. Eng.*, 2016, **10**, 1121.
9 R. Nassar, A. Trivella, S. Mokh, M. Al-Iskandarani, H. Budzinski and P. Mazellier, *J. Photochem. Photobiol., A*, 2017, **336**, 176.
10 F. J. Real, F. J. Benitez, J. L. Acero, G. Roldan and F. Casas, *J. Chem. Technol. Biotechnol.*, 2016, **91**, 1004.
11 P. Calza, V. A. Sakkas, A. Villioti, C. Massolino, V. Boti, E. Pelizzetti and T. Albanis, *Appl. Catal., B*, 2008, **84**, 379.
12 C. Garcıa, R. Oyola, L. Piñero, D. Hernández and R. Arce, *J. Phys. Chem. B*, 2008, **112**, 168.
13 Y. Chen, J. Liang, L. Liu, X. Lu, J. Deng, I. P. Pozdnyakov and Y. Zuo, *J. Environ. Qual.*, 2017, **46**, 1081.
14 Y. Chen, C. Hu, X. Hu and J. Qu, *Environ. Sci. Technol.*, 2009, **43**, 2760.
15 M. P. Makunina, I. P. Pozdnyakov, Y. Chen, V. P. Grivin, N. M. Bazhin and V. F. Plyusnin, *Chemosphere*, 2015, **119**, 1406.
16 E. D. Mordvinova, M. V. Parkhats, Y. Chen and I. P. Pozdnyakov, *Mendeleev Commun.*, 2019, **29**, 426.
17 I. P. Pozdnyakov, V. F. Plyusnin, V. P. Grivin, D. Yu. Vorobyev, N. M. Bazhin and E. Vauthey, *J. Photochem. Photobiol., A*, 2006, **181**, 37.
18 C. Weller, S. Horn and H. Herrmann, *J. Photochem. Photobiol., A*, 2013, **255**, 41.
19 G. V. Buxton, C. L. Greenstock, W. P. Helman and A. B. Ross, *J. Phys. Chem. Ref. Data*, 1988, **17**, 513.
20 P. M. Hare, E. A. Price and D. M. Bartels, *J. Phys. Chem. A*, 2008, **112**, 6800.

Received: 19th May 2020; Com. 20/6221